Biochemical and Biophysical Research Communications 374 (2008) 169–174

Contents lists available at ScienceDirect

Biochemical and Biophysical Research Communications

journal homepage: www.elsevier.com/locate/ybbrc

Design and kinetic analysis of hammerhead ribozyme and DNAzyme that specifically cleave *TEL–AML1* chimeric mRNA

Woo-Hyung Choi [a,1], Bo-Ra Choi [a,1], Jae Hyun Kim [b], Woon-Seok Yeo [a], Sangtaek Oh [c], Dong-Eun Kim [a,*]

[a] Department of Bioscience and Biotechnology, Konkuk University, 1-Hwayang-dong, Gwangjin-gu, Seoul 143-701, Republic of Korea
[b] Nambu Blood Laboratory, Korean Red Cross, Busan 614-814, Republic of Korea
[c] PharmcoGenomic Research Center, Inje University, Busan 614-735, Republic of Korea

ARTICLE INFO

Article history:
Received 2 July 2008
Available online 15 July 2008

Keywords:
Acute lymphoblastic leukemia
Hammerhead ribozyme
Oligodeoxyribozyme
TEL–AML1 fusion

ABSTRACT

In order to develop the oligonucleotides to abolish an expression of *TEL–AML1* chimeric RNA, which is a genetic aberration that causes the acute lymphoblastic leukemia (ALL), hammerhead ribozymes and deoxyoligoribozymes that can specifically cleave *TEL–AML1* fusion RNA were designed. Constructs of the deoxyribozyme with an asymmetric substrate binding arm (Dz26) and the hammerhead ribozyme with a 4 nt-bulged substrate binding arm in the stem III (buRz28) were able to cleave *TEL–AML1* chimeric RNA specifically at sites close to the junction *in vitro*, without cleaving the normal *TEL* and *AML1* RNA. Single-turnover kinetic analysis under enzyme-excess condition revealed that the buRz28 is superior to the Dz26 in terms of substrate binding and RNA-cleavage. In conjunction with current progress in a gene-delivery technology, the designed oligonucleotides that specifically cleave the *TEL–AML1* chimeric mRNA are hoped to be applicable for the treatment of ALL *in vivo*.

The hammerhead ribozyme is the smallest naturally occurring ribozyme identified, which is capable of performing sequence-specific cleavage of RNA [1], and is widely employed for inhibiting the function of target genes [2–4]. Functional hammerhead ribozyme can be designed to cleave any target RNA *in trans* by generating RNA molecules with sequences reverse complementary to a target RNA in the hybridizing arms that flank a functional ribozyme core sequence [5,6]. The trans-acting hammerhead ribozyme can cleave any target substrate containing a 5′-NUH-3′ triplet (where N represents any nucleotide and H represents A, C, or U) [7–11] (box in Fig. 1). Complementary sequences generally constitute 14–16 nucleotides in total, spanning on both sides of the target site selected [12]. This is thought to allow sufficient specificity for the cleavage reaction while conferring a ready dissociation from the target, which is typically the rate-limiting step in the catalytic cycle [13,14]. RNA-cleaving deoxyribozymes, which are capable of sequence-specific cleavage of target mRNA, have been discovered through the *in vitro* selection technology [15]. The "10–23" RNA-cleaving deoxyribozyme or DNAzyme can recognize RNA through Watson–Crick base-pairing, and cleaves its target at a phosphodiester bond located between an unpaired purine (R) and pyrimidine (Y) (box in Fig. 1).

Acute lymphoblastic leukemia (ALL) that is often found in childhood hematopoietic malignancies is associated with the chromosomal translocation between chromosomes 12 and 21 [16]. The chromosomal translocation t(12;21)(p12;q22) results in the formation of the *TEL–AML1* fusion gene that encodes a chimeric protein, TEL–AML1, which contains the 336 amino-terminal region of TEL that is an ETS-like putative transcription factor fused to the residues 21–480 of tissue-specific transcription factor, AML1 [16–18]. Since TEL and AML1 are putative transcription factors, it has been suggested that the acquisition of the t(12;21) alters the regulation of hematopoietic-specific gene expression that results in unregulated growth of leukemic cells. It has been observed that the TEL–AML1 fusion protein encoded by the *TEL–AML1* chimeric mRNA is unique to the malignant cell phenotype and is primarily responsible for leukemogenesis [16,19].

In this study, we have designed hammerhead ribozyme and 10–23 DNAzyme that specifically targets the junction sequence and cleave chimeric *TEL–AML1* mRNA, not disrupting normal mRNAs that share part of the chimeric RNA. We compared the designed hammerhead ribozymes and 10–23 DNAzymes with a respect to kinetics and efficiencies of *TEL–AML1* chimeric mRNA-cleavage *in vitro*.

Materials and methods

Preparation of DNAzymes, hammerhead ribozymes, and substrate RNAs. The 10–23 DNAzymes (Fig. 1) and DNA templates for RNA

* Corresponding author. Fax: +82 2 3436 6062.
E-mail address: kimde@konkuk.ac.kr (D.-E. Kim).
[1] Both the authors contributed equally to this work.

0006-291X/$ - see front matter © 2008 Elsevier Inc. All rights reserved.
doi:10.1016/j.bbrc.2008.07.008

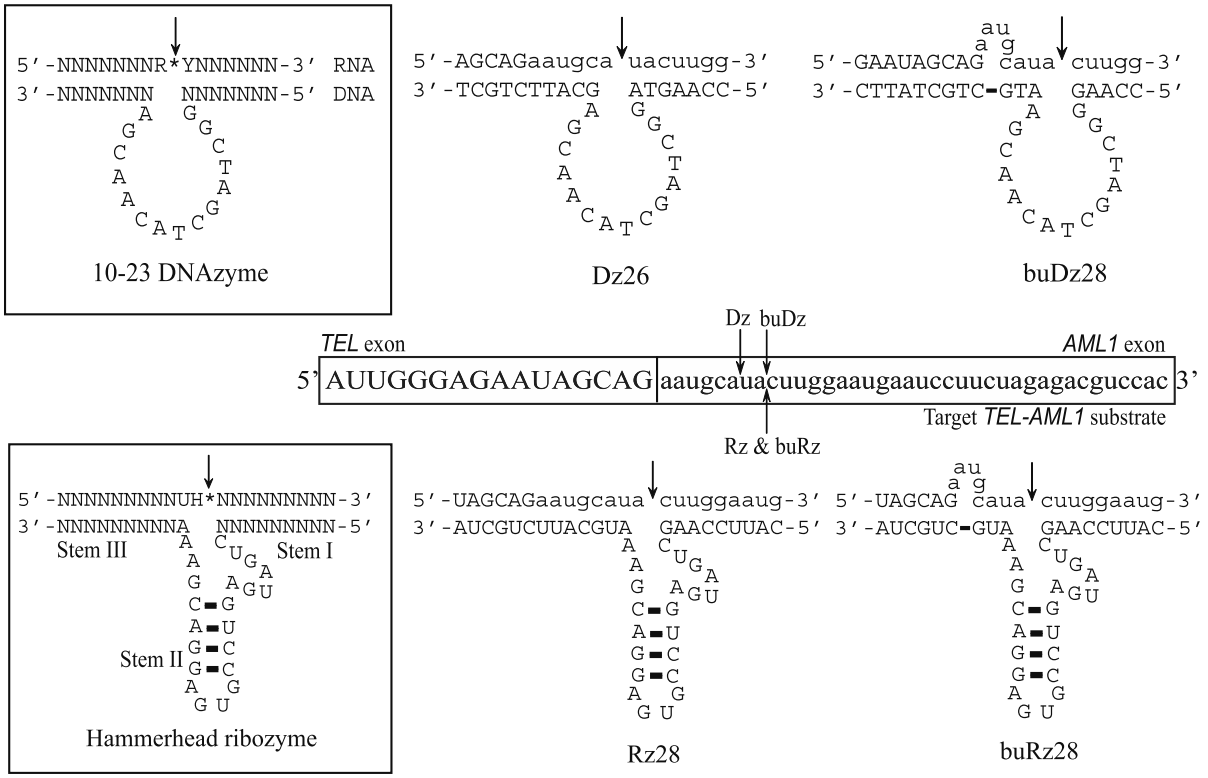

Fig. 1. Nucleotide sequences of the designed DNAzymes and hammerhead ribozymes targeted to the *TEL–AML1* chimeric RNA. The sequence of *TEL–AML1* near the junction is shown. The *TEL* exon sequence near the junction is depicted by capital letters and *AML1* exon sequence is shown in lowercase letters. Potential sites of cleavage by the constructed DNAzymes and ribozymes are indicated by arrows.

synthesis were chemically synthesized (Cosmo Gentech, Seoul, Korea). All oligodeoxynucleotides were purified by denaturing polyacrylamide gel electrophoresis (PAGE). Hammerhead ribozymes were also prepared by chemical synthesis (Bioneer Co., Daejeon, Korea). DNA templates for *TEL–AML1* substrate RNA and for both the normal *TEL* and *AML1* substrate RNAs were synthesized chemically. DNA templates for the *in vitro* synthesis of RNAs contained the antisense sequence of T7 promoter and respective RNA sequence. Downstream of the promoter sequence, GG residues at 5′-side were inserted for higher efficiency of transcription. Reaction mixture and the annealing primer for the transcription was prepared as reported [20].

Test of target RNA-cleavage with DNAzymes and ribozymes. Triphosphate groups from the 5′-end of the substrates RNA were removed with calf intestinal alkaline phosphatase and the dephosphorylated transcripts were then labeled using T4 polynucleotide kinase and [γ-^{32}P]ATP (6000 Ci/mmol, GE Healthcare). 5′-end labeled substrate RNAs were purified by denaturing PAGE. All target RNA-cleavage activities of ribozymes and DNAzymes were tested in the reaction buffer (20 mM $MgCl_2$ and 20 mM TrisHCl, pH 7.5) under single-turnover (enzyme-saturating) conditions at 37 °C. The reaction was initiated by combining a trace amount of ^{32}P-5′-labeled substrate RNA that was mixed with each unlabeled corresponding substrate (to yield final concentration of 50 nM RNA) and each enzyme (ribozyme or DNAzyme, 500 nM final concentration), which were separately heated to 85 °C for 2 min followed by cooling to 37 °C for 10 min to disrupt potential aggregates prior to the reaction, in the buffer containing 20 mM $MgCl_2$. The reactions were quenched by adding an equal volume of the gel-loading buffer containing 25 mM Na_2EDTA and 8 M urea. The products were resolved by 15% (w/v) denaturing PAGE containing 8 M urea. The product bands were visualized and quantified on Cyclone PhosphorImager (Packard Instruments, Meriden, CT).

Single-turnover kinetics of RNA-cleavage reaction. The RNA-cleavage reaction was performed under pseudo-unimolecular reaction condition, where [E] >> [S] and the [E] is hardly affected by the reaction, at 37 °C. 3 nM of target RNA substrate was mixed with increasing concentration (10–500 nM) of DNAzyme or ribozyme, and the time-courses of RNA-cleavage were measured. To follow the RNA-cleavage time-course, aliquots of reaction mixture were withdrawn at various times and quenched by adding an equal volume of the gel-loading buffer. ^{32}P-labeled substrates and products of the quenched reaction were separated by 15% (w/v) denaturing PAGE containing 8 M urea, and were detected and quantified as described above. Kinetics of RNA-cleavage reaction was fitted to a single-exponential equation to obtain the overall rate of RNA-cleavage reaction (k_{obs}); $Y = \mathrm{Amp} \cdot [1 - \exp(-k_{obs} \cdot t)]$, where Y and Amp represents a fraction of RNA cleaved and its amplitude at infinite time of reaction, respectively. Differentiation of the single-exponential function with a time provides an initial velocity of the reaction at time zero as a form of $\mathrm{Amp} \cdot k_{obs}$. The initial velocities were plotted against [E] to obtain rates of association (k_1) of the enzyme and the substrate. The obtained initial velocities of RNA-cleavage reaction that were hyperbolically increased were fit to a hyperbolic equation, $k_{obs} = k_{max} \cdot [E]/(K_{1/2} + [E])$ to yield k_{max} and $K_{1/2}$, which in turn provides a $k_{max}/K_{1/2}$ value that represents a lower limit of apparent rate of association (k_1) in the following kinetic pathway;

$$E + S \underset{k_{-1}}{\overset{k_1}{\rightleftharpoons}} E{:}S \xrightarrow{k_2} E{:}P$$

The rate constant for cleavage within the enzyme–substrate complex (k_2) was measured as following method; the enzyme (500 nM of DNAzyme or ribozyme) and the substrate (3 nM) were heat-treated in the reaction buffer without Mg^{2+} at 85 °C for

2 min, allowed to anneal 30 min at 37 °C, and the reaction was initiated by supplementing $MgCl_2$ (final concentration of 20 mM).

Pulse-chase kinetics of RNA-cleavage reaction. Rates of the enzyme–substrate complex dissociation (k_{-1}) were determined by a pulse-chase experiment. The RNA-cleavage reaction was initiated by mixing DNAzyme or ribozyme (500 nM) with radioactive RNA substrate (less than 1 nM) in the reaction buffer at 37 °C. After 1 min the reaction mixture was subsequently chased with nonradioactive RNA substrate (1.0 μM in the same buffer as above). At various intervals after addition of the chase RNA substrate, aliquots of reaction mixture were withdrawn and quenched with the gel-loading buffer. ^{32}P-labeled substrates and products of the quenched reaction were separated by 15% (w/v) denaturing PAGE/8 M urea, and were detected and quantified as described above. A parallel reaction was carried out without the chase, and its kinetics of the RNA-cleavage reaction was compared with the RNA-cleavage reaction performed with the RNA chase. The rate constant for substrate dissociation, k_{-1}, was calculated from the fraction of substrate that goes on for RNA-cleavage after the chase period [21].

Results and discussion

Design of hammerhead ribozyme and DNAzyme targeting the chimeric TEL–AML1 RNA

Antisense molecules that are directed against two non-contiguous sequences necessitate the specificity to discriminate the chimeric RNA substrate from the non-target sequences, as exemplified in the case of *bcr-abl* sequence [22]. In *TEL–AML1* chimeric RNA one potential target site (28 nt away from 5′-end of the *AML1*) for a hammerhead ribozyme was chosen within 10 nt of the junction (Fig. 1); the Rz28 was designed to cleave the *TEL–AML1* chimeric RNA substrate at the AUA triplet located 8 nt 3′ of the junction. In this construct, length of the stem III is longer than that of the stem I in order to encompass two non-contiguous fusion sequences, resulting in an asymmetric substrate annealing arm. Other version of ribozyme targeting the same site was also constructed, in which one annealing arm (stem III) was designed to generate 4 nt bulge when annealed to the *TEL–AML1* chimeric RNA substrate (buRz28). The buRz28 covers to the same extent of sequence as does the Rz28 in the substrate binding, but it has a symmetric binding arm that anneals with 9 nt of the substrate in each side.

Two potential RNA-cleavage sites for DNAzyme were chosen; the AU and AC doublet located 6- and 8 nt 3′ of the junction, respectively, which are close to the cleavage site for ribozyme. Two DNAzymes containing the 10–23 catalytic motif and designated length of hybridizing arms specific for each site along the target RNA of *TEL–AML1* were constructed (Fig. 1). The hybridizing arms of the DNAzymes were designed to specifically recognize both segments of *TEL* and *AML1* gene flanking the *TEL–AML1* junction to discriminate the target *TEL–AML1* chimeric mRNA from the normal *TEL* and *AML1* mRNA. One DNAzymes was designed to contain 4 nt bulge in binding arm (buDz28), because the potential

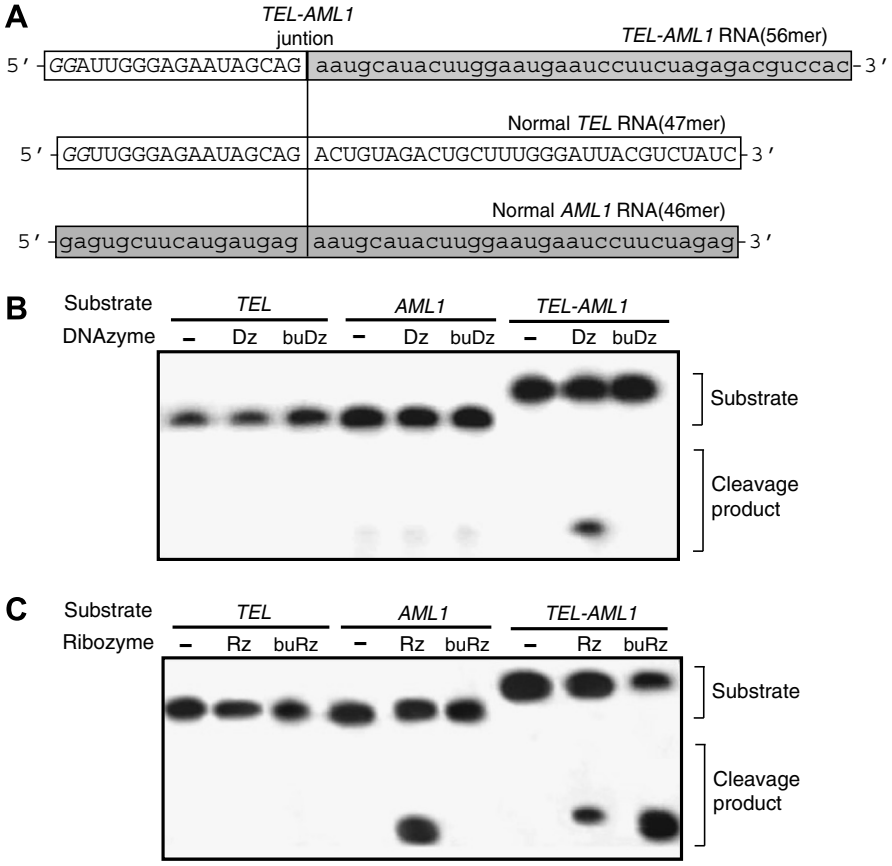

Fig. 2. Specificity in target RNA-cleavage by the constructed DNAzymes and hammerhead ribozymes. (A) Three RNA substrates were used to examine specificity of the target RNA-cleavage. For efficient RNA synthesis by the T7 RNA polymerase, two G nucleotides (*GG*) were introduced at the 5′-end of *TEL* and *TEL–AML1* RNAs. (B) Cleavage of the *TEL–AML1* substrate by the Dz26 generated a visible 5′ fragment of 24 nts, whereas the buDz26 was unable to cleave any RNA substrates. No cleavage of the normal RNAs by the Dz26 was observed. (C) The Rz28 cleaved the chimeric *TEL–AML1* as well as the normal *AML1* RNA. The buRz28 cleaved only the *TEL–AML1* substrate without cleavage of the normal RNA substrates.

cleavage site was relatively distal from the junction (8 nt away) compared with cleavage sites for the other DNAzyme (Dz26).

Specificity and catalytic activity of the designed DNAzymes and ribozymes

In order to examine the specificity of cleavage reactions catalyzed by the designed DNAzymes and the ribozymes, we investigated RNA-cleavage activity and specificity against the chimeric *TEL–AML1* RNA substrate and the normal *TEL* and *AML1* substrates. Enzymes with high specificity should cleave only the chimeric *TEL–AML1* RNA substrate. Substrate *TEL–AML1* chimeric RNA consisted of the sequence from 16 nt 5′ of the *TEL–AML1* junction to 38 nt 3′ of the *TEL–AML1* junction (Fig. 2A). Containing the *TEL–AML1* breakpoint (1033 nt of *TEL* and 58 nt of *AML1* coding sequence) in the middle, the region of the normal *TEL* substrate RNA extended from position 1019 to 1063 of normal *TEL* cDNA, and the normal *AML1* substrate RNA extended from position 42 to 87 of normal *AML1* cDNA (Fig. 2A). One DNAzyme (Dz26) exhibited a specific cleavage of the chimeric *TEL–AML1* substrate, but the other construct (buDz28) could not cleave any RNA substrate (Fig. 2B). This result indicates that the bulge introduced near the cleavage site in the DNAzyme–substrate complex abolished a catalytic activity of the enzyme. We are currently investigating the effect of bulge in the DNAzyme–RNA substrate construct on the RNA-cleavage activity, regarding to the closeness of the bulge to the cleavage site and a size of the bulge in the construct.

In contrast, both ribozymes efficiently cleaved the *TEL–AML1* substrate at the anticipated sites, but the Rz28 showed a promiscuous activity by cleaving the chimeric RNA as well as the normal substrate (*AML1*) (Fig. 2C). Moreover, the amount of cleavage product obtained from the normal *AML1* RNA with the Rz28 ribozyme was comparable to that obtained from the chimeric *TEL–AML1* substrate. This result indicates that the designed ribozymes, with their relatively long antisense arms, recognized not only the chimeric *TEL–AML1* RNA but also the normal *AML1* RNA as substrate. However, the buRz28 ribozyme was able to retain the catalytic activity with substrate specificity. Recently, crystal structure of the full-length hammerhead ribozyme has been elucidated with a conjecture of tertiary contacts important for enhanced catalysis, in which tertiary interaction between the stem I bulge and stem II loop is believed to be important to attain the catalytic activity [23]. Not mutually exclusive to this observation, we have found that the stem III bulge/stem II loop interaction is also tolerable for the hammerhead ribozyme to retain RNA-cleavage activity, as demonstrated by unhampered activity of the buRz28 harboring the bulged structure in the stem III.

Single-turnover RNA-cleavage kinetics of DNAzyme Dz26 and hammerhead ribozyme buRz28

To compare the cleavage activity of the ribozyme and the DNAzyme in detail, we determined the single-turnover kinetic parameters for the cleavage of the *TEL–AML1* RNA substrate. The RNA-cleavage reactions with the selected enzymes (Dz26 and buRz28) were performed in 20 mM $MgCl_2$ under enzyme-saturating conditions at 37 °C. As shown in Fig. 3A, fraction of the product formed by the ribozyme followed a single-exponential kinetics. Differentiation of the single-exponential function with a time provides an initial velocity of the reaction at time zero, and the initial velocities were plotted against [Ribozyme] (*inset* in Fig. 3A). The initial velocities were fit to the hyperbolic equation ($k_{obs} = k_{max} \cdot [E]/(K_{1/2} + [E])$; [E] stands for the ribozyme concentration) to provide a $k_{max}/K_{1/2}$ value of $7.1 \times 10^6\ M^{-1}\ min^{-1}$, which is equal to a lower limit for the substrate association rate, k_1. The hyperbolic dependency of the observed rate for RNA-cleavage reaction

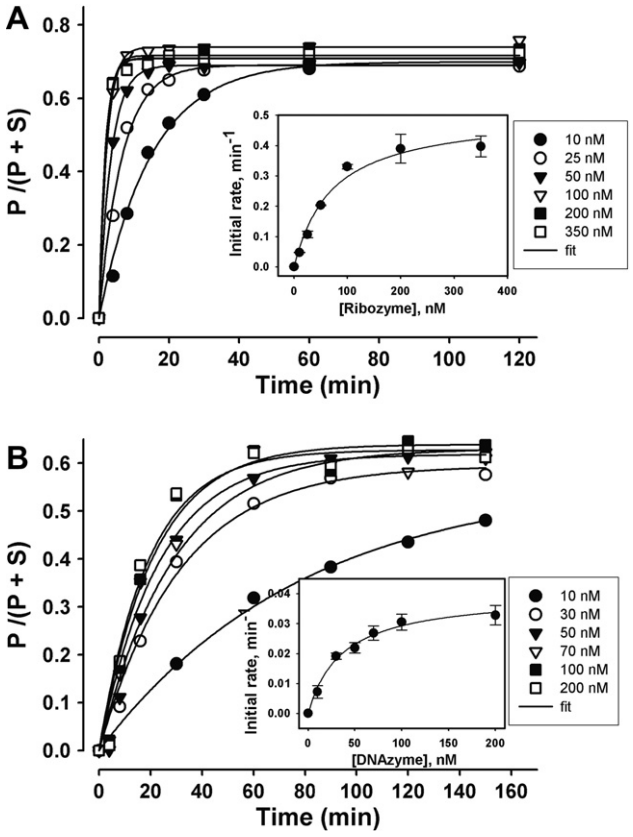

Fig. 3. Single-turnover kinetics for Dz26- and buRz28-mediated RNA-cleavage. (A) Various concentrations of buRz28 ribozyme were mixed with the *TEL–AML1* substrate at 37 °C. Single-turnover kinetics of RNA-cleavage reaction was fitted to a single-exponential equation to obtain the observed rate of RNA-cleavage reaction (continuous lines). *Inset*; The observed initial velocities of RNA-cleavage by the buRz28 were fit to the hyperbolic equation, $k_{obs} = k_{max} \cdot [E]/(K_{1/2} + [E])$ to yield $k_{max} = 0.51\ min^{-1}$ and $K_{1/2} = 71.5$ nM. (B) The same kinetic analysis was carried out for the DNAzyme, Dz26. *Inset*; hyperbolic fit (continuous line) to the initial velocities versus [E] provides $k_{max} = 0.040\ min^{-1}$ and $K_{1/2} = 36.6$ nM.

provides an evidence for a conformational change and/or RNA-cleavage step (*i.e.* chemistry step) with an apparent rate of $0.51\ min^{-1}$(k_{max}), following the bimolecular encounter between the ribozyme and RNA substrate.

Similarly, the DNAzyme (Dz26) also followed an exponential kinetics of RNA-cleavage (Fig. 3B), and a plot of the observed initial rates of RNA-cleavage versus increasing concentrations of DNAzyme showed a hyperbolic dependency (*inset* in Fig. 3B). The hyperbolic increase of the rate constants with a plateau of about $0.04\ min^{-1}$ (k_{max}) indicates that a conformational change and/or RNA-cleavage step occurs at an apparent rate of $0.040\ min^{-1}$, following the association of the DNAzyme into the RNA substrate. The hyperbolic fit provided an apparent rate of substrate association by the DNAzyme, $k_1 = 1.1 \times 10^6\ M^{-1}\ min^{-1}$, which is 6.5-times slower than that of the ribozyme. Note that the apparent rates of substrate binding and RNA-cleavage represent lower limit of each individual step, in which individual rate constants dictate the apparent rate of the given step. Therefore, we set out the experiments to determine the individual rates for the RNA-cleavage (k_2) and the substrate dissociation (k_{-1}).

The rate constant for cleavage within the enzyme–substrate complex (k_2) in the kinetic pathway was measured as outlined in Fig. 4A. The RNA-cleavage kinetics in this method was compared with the RNA-cleavage kinetics obtained by the normal way of mixing in the presence of 20 mM $MgCl_2$, where the RNA-cleavage was started by mixing the DNAzyme and the substrate. The

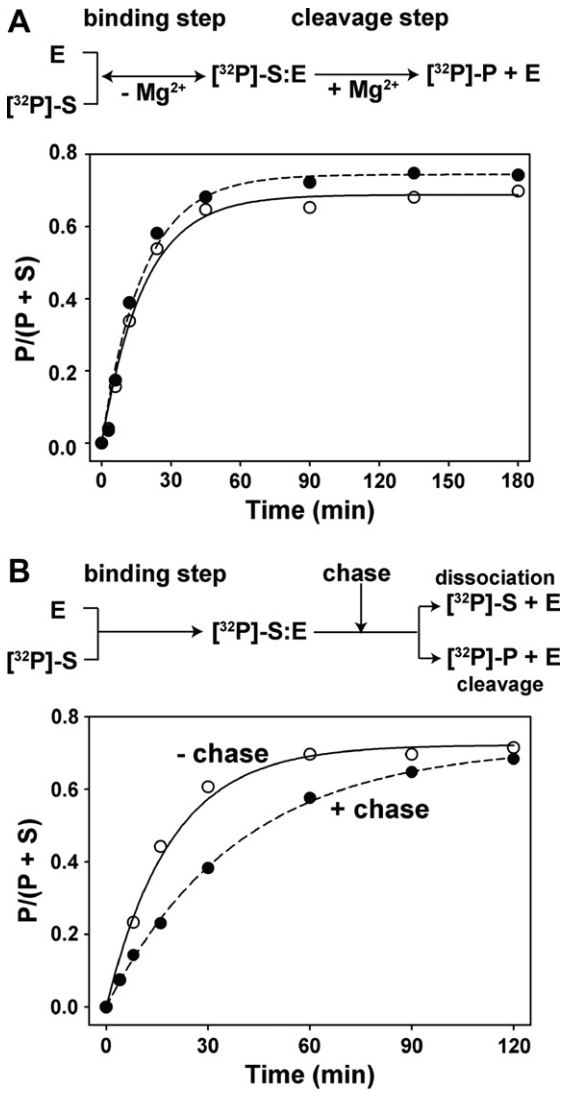

Fig. 4. Determination of the rate of RNA-cleavage (k_2) and substrate dissociation (k_{-1}) for Dz26. (A) The rate constant for RNA-cleavage within the enzyme–substrate complex (k_2) was measured as outlined in the experimental scheme shown above the graph. Time-courses of RNA-cleavage was plotted (●) and fitted to an exponential function to get a rate of 0.055 min^{-1}. A parallel reaction was performed, where the RNA-cleavage was started by mixing the enzyme and the substrate in the presence of Mg^{2+} (○), and fitted to an exponential function to get a rate of 0.056 min^{-1}. (B) The pulse-chase reaction to determine the rate of substrate dissociation was performed as outlined in the experimental scheme shown above the graph. Time-courses of the chased reaction (●) was fitted to an exponential function, yielding a rate of 0.0527 min^{-1}. A parallel reaction was carried out without the chase (○), and fitted to an exponential function to yield a rate of 0.0254 min^{-1}.

observed rate of RNA-cleavage in both cases was very close to each other (k_{obs} = 0.055 and 0.056 min^{-1} for Mg^{2+}-supplied and Mg^{2+}-deficient condition, respectively), confirming that the substrate binding did not affect the observed rate for the k_2 measurement. The observed rate of 0.056 min^{-1} represents a more reliable rate of RNA-cleavage (the chemistry step) than the rate obtained from the hyperbolic fit (k_{max} of 0.040 min^{-1} in Fig. 3B), because under this experimental set-up the observed rate of RNA-cleavage solely reflects the chemistry step within the enzyme–substrate complex. These results suggest that the Dz26 undergoes substrate dissociation prior to the RNA-cleavage because the maximum observed rate of RNA-cleavage (k_{max}) in Fig. 3B exhibited a significantly slower rate than the k_2. However, in the case of the buRz28 the rate constant for RNA-cleavage within the ribozyme–substrate complex (k_2 = 0.53 min^{-1}, data not shown) obtained by the same method was very close to the one obtained with the hyperbolic fit (k_{max} of 0.51 min^{-1} in Fig. 3B), indicating that the buRz28 shows very few dissociation events in the enzyme–substrate complex.

Due to a possibility that the Dz26 may dissociate from the substrate RNA before RNA-cleavage reaction, it was necessary to measure the dissociation rate of the DNAzyme:substrate complex. As outlined in Fig. 4B, a pulse-chase experiment was designed to obtain upper limit for substrate dissociation rate (k_{-1}). This method monitors the partitioning of a DNAzyme:substrate complex between RNA-cleavage and substrate dissociation. The pulse-chase experiment was carried out for the Dz26 as described in "Materials and methods" section. Under this condition, dissociation of labeled substrate is irreversible, and thus the accumulation of product over time in the chase step represents competition between cleavage and substrate dissociation. As shown in Fig. 4B, the chased reaction exhibited an observed rate of RNA-cleavage of 0.0254 min^{-1}, which is slower than the rate obtained without the chase (0.0527 min^{-1}). The rate of dissociation was calculated to be 0.059 min^{-1} from the relationship k_{obs} (chase)/k_{obs} (control) = $k_2/(k_2 + k_{-1})$ [21], indicating that the substrate dissociation rate is comparable to the rate of chemistry step. In contrast, the buRz28 did not show a slowed chase rate as compared to the rate obtained without the chase (Supplementary Fig. 1). This result corroborates that the buRz28 rarely dissociate from the substrate before the RNA-cleavage.

Furthermore, we have observed that the buRz28 and the Dz26 significantly decreased a protein expression of the leukemogenic *TEL–AML1* gene, which was introduced into the cells, as shown in the Western analysis (Supplementary Fig. 2). Therefore, as indicated in the RNA-cleavage experiments, it is feasible to apply both the selected DNAzyme and ribozyme for a selective inactivation of the leukemogenic *TEL–AML1* gene in the cells. As a therapeutic agent, antisense catalytic oligonucleotides such as DNAzymes and ribozymes have obvious advantageous properties as compared with the RNA interference (RNAi)-based drugs. Since these oligonucloetides do not utilize the cellular machinery to destroy the target RNA, they can avoid the issues of exploiting the cellular RNAi factors. Although the RNAi is a very powerful tool for gene inactivation *in vivo*, it has been reported that transfection of short-interfering (si) RNAs triggers the interferon-mediated innate immune response [24]. In contrast, the oligonucleotide-based drugs that are easy to formulate and to be chemically modified can evade the innate immune response of the host. Clinically, these oligonucleotide-based regimens have been tried against viral infection and cancers [4,25]. In conjunction with current progress in a nucleic acid delivery technology, which is a bottleneck for a development of oligonucleotide-based gene therapy, our designed oligonucleotides that cleave the chimeric mRNA are hoped to be developed into the effective drug candidates to treat the ALL.

Acknowledgments

This research was supported by the Korea Science and Engineering Foundation (KOSEF) Grant funded by the Korea government (MOST) (R01-2006-000-10617-0) and the Korea Research Foundation Grant funded by the Korean government (MOEHRD, Basic Research Promotion Fund) (KRF-2006-312-C00594).

Appendix A. Supplementary data

Supplementary data associated with this article can be found, in the online version, at doi:10.1016/j.bbrc.2008.07.008.

References

[1] R.H. Symons, Small catalytic RNAs, Annu. Rev. Biochem. 61 (1992) 641–671.
[2] M. Amarzguioui, H. Prydz, Hammerhead ribozyme design and application, Cell. Mol. Life Sci. 54 (1998) 1175–1202.
[3] K.R. Birikh et al., Probing accessible sites for ribozymes on human acetylcholinesterase RNA, RNA 3 (1997) 429–437.
[4] L.Q. Sun et al., Catalytic nucleic acids: from lab to applications, Pharmacol. Rev. 52 (2000) 325–347.
[5] O.C. Uhlenbeck, A small catalytic oligoribonucleotide, Nature 328 (1987) 596–600.
[6] J. Haseloff, W.L. Gerlach, Simple RNA enzymes with new and highly specific endoribonuclease activities, Nature 334 (1988) 585–591.
[7] M. Koizumi, S. Iwai, E. Ohtsuka, Cleavage of specific sites of RNA by designed ribozymes, FEBS Lett. 239 (1988) 285–288.
[8] D.E. Ruffner et al., Sequence requirements of the hammerhead RNA self-cleavage reaction, Biochemistry 29 (1990) 10695–10702.
[9] R. Perriman, A. Delves, W.L. Gerlach, Extended target-site specificity for a hammerhead ribozyme, Gene 113 (1992) 157–163.
[10] T. Shimayama et al., Extraordinary enhancement of the cleavage activity of a DNA-armed hammerhead ribozyme at elevated concentrations of Mg^{2+} ions, FEBS Lett. 368 (1995) 304–306.
[11] M. Zoumadakis, M. Tabler, Comparative analysis of cleavage rates after systematic permutation of the NUX consensus target motif for hammerhead ribozymes, Nucleic Acids Res. 23 (1995) 1192–1196.
[12] T.C. Jarvis et al., Site selection and chemical modifications of ribozymes targeting the proto-oncogene c-myb, J. Biol. Chem. 271 (1996) 29107–29112.
[13] J. Goodchild, V. Kohli, Ribozymes that cleave an RNA sequence from human immunodeficiency virus: the effect of flanking sequence on rate, Arch. Biochem. Biophys. 284 (1991) 386–391.
[14] P. Hendry, M. McCall, Unexpected anisotropy in substrate cleavage rates by asymmetric hammerhead ribozymes, Nucleic Acids Res. 24 (1996) 2679–2684.
[15] S.W. Santoro, G.F. Joyce, A general purpose RNA-cleaving DNA enzyme, Proc. Natl. Acad. Sci. USA 94 (1997) 4262–4266.
[16] T.R. Golub et al., Fusion of the TEL gene on 12p13 to the AML1 gene on 21q22 in acute lymphoblastic leukemia, Proc. Natl. Acad. Sci. USA 92 (1995) 4917–4921.
[17] S.P. Romana et al., High frequency of t(12;21) in childhood B-lineage acute lymphoblastic leukemia, Blood 86 (1995) 4263–4269.
[18] S.P. Romana et al., The t(12;21) of acute lymphoblastic leukemia results in a tel-AML1 gene fusion, Blood 85 (1995) 3662–3670.
[19] J.K. Rho et al., Correlation between cellular localization of TEL/AML1 fusion protein and repression of AML1-mediated transactivation of CR1 gene, Biochem. Biophys. Res. Commun. 297 (2002) 91–95.
[20] D.E. Kim, G.F. Joyce, Cross-catalytic replication of an RNA ligase ribozyme, Chem. Biol. 11 (2004) 1505–1512.
[21] M.J. Fedor, O.C. Uhlenbeck, Kinetics of intermolecular cleavage by hammerhead ribozymes, Biochemistry 31 (1992) 12042–12054.
[22] R. Kronenwett et al., Kinetic selectivity of complementary nucleic acids: bcr-abl-directed antisense RNA and ribozymes, J. Mol. Biol. 259 (1996) 632–644.
[23] M. Martick, W.G. Scott, Tertiary contacts distant from the active site prime a ribozyme for catalysis, Cell 126 (2006) 309–320.
[24] C.A. Sledz et al., Activation of the interferon system by short-interfering RNAs, Nat. Cell Biol. 5 (2003) 834–839.
[25] B.A. Sullenger, E. Gilboa, Emerging clinical applications of RNA, Nature 418 (2002) 252–258.